Journal of Renewable Energy and Environment

Journal Homepage: www.jree.ir

Materials and Energy Research Center

MERC

Research Article

Performance Evaluation and Optimization of a Solar-Assisted Multi-Belt Conveyor Dryer Based on Response Surface Methodology

Hemad Zareiforoush *, Adel Bakhshipour, Iraj Bagheri

Department of Biosystems Engineering, Faculty of Agriculture, University of Guilan, P. O. Box: 41635-1314, Rasht, Guilan, Iran.

PAPER INFO

Paper history:
Received: 08 June 2021
Revised in revised form: 25 August 2021
Scientific Accepted: 25 September 2021
Published: 29 December 2021

Keywords:
Drying,
Specific Energy,
Energy Efficiency,
Solar-Assisted Dryer,
Solar Water Heater

ABSTRACT

Drying process is an important post-harvest stage of food crops production which accounts for about 20 % of the world's energy consumption in the industrial sector. One of the effective ways to reduce the share of fossil fuel consumption in the food drying process is to develop new drying systems based on the use of renewable energy sources. In this research, a novel solar-assisted multi-belt conveyor dryer was developed and its performance was analysed. The required thermal energy for drying process was supplied by the combination of solar-gas water heaters and four solar-powered infrared (IR) lamps. The experimental factors included the speed and temperature of the drying air and the power of IR lamps. The performance characteristics were drying time, Overall Specific Energy (OSE), Non-Solar Specific Energy (NSE), Overall Energy Efficiency (OEE), and Solar-Assisted Energy Efficiency (SEE). The optimization process of the drying system was carried out using Response Surface Methodology (RSM) by defining two general modes for the energy sources of the drying system, namely overall mode and solar-assisted mode. Based on the results, the lowest OSE (17.30 MJ/kg water evaporated) was obtained when the speed and temperature of the drying air were equal to 7 m/s and 40 °C, respectively, without using IR power. The lowest NSE (2.71 MJ/kg water evaporated) was achieved by applying the treatment of 7 m/s * 40 °C * 300 W. The maximum OEE was equal to 13.92 % whilst the maximum SEE was obtained as 88.71 %. Both of the mentioned maximum values were obtained at the speed and temperature combination of 7 m/s and 40 °C and their difference was applying 300 W IR power to gain maximum SEE and no IR utilization for the maximum OEE. According to RSM analysis, the optimum working conditions for the drying system included the treatment of 7 m/s * 39.96 ºC * 300 W. Under this condition, the drying time, NSE, and SEE values were equal to 180.95 min, 1.062 MJ/kg water evaporated, and 84.63 %, respectively.

https://doi.org/10.30501/jree.2021.285697.1203

1. INTRODUCTION

Global developments in the field of environmental protection and the depletion of fossil fuel sources are accelerating the trend towards the use of renewable energy and are attracting much more attention in the world. Reduction of fossil energy sources along with population and economic growth and increasing air and environment pollution make it necessary to use renewable energy sources according to their economic justification.

Since the moisture content of fresh food and agricultural crops is often high, drying operations are required to remove the excess water to preserve the quality and durability of the products during their storage. Drying process is an important post-harvest stage of food crops production with a considerable energy consumption. About twenty percent of the world's energy consumption in the industrial sector is related to the drying process [1, 2]. Depending on the type and quality of food that should be dehydrated, several methods have been developed over time to dry the products [3]. During the drying process, significant amounts of thermal energy are consumed and in most cases, the type of energy used in the drying process is fossil fuel [4].

One of the most potential applications of dryers is to dehydrate medicinal herbs. This is because of the several benefits of medicinal herbs for human health and that most of these plants are not available in fresh form throughout the year. Consequently, they must be dried to be available at any time of the year. Since the qualitative characteristics of medicinal plants such as microbial activity constituents can be significantly affected by the drying treatment and environmental conditions, they must often be dried immediately after harvesting from the farm [5]. It has been proved that traditional methods like open sun drying have many disadvantages and negative effects on the quality of products because of uncontrolled heat transfer and low drying rate. On the other hand, biomass-based and infrared drying methods are accompanied with high cost, high levels of fossil fuel consumption, and environmental pollution [6]. It has been

*Corresponding Author's Email: hemad.zareiforoush@guilan.ac.ir (H. Zareiforoush)
URL: https://www.jree.ir/article_142561.html

Please cite this article as: Zareiforoush, H., Bakhshipour, A. and Bagheri, I., "Performance evaluation and optimization of a solar-assisted multi-belt conveyor dryer based on response surface methodology", ***Journal of Renewable Energy and Environment (JREE)***, Vol. 9, No. 1, (2022), 78-92. (https://doi.org/10.30501/jree.2021.285697.1203).

reported that the quality and medicinal value of stevia leaves can be remarkably degraded by open sun drying. Considering the aforementioned challenges, solar drying can be a good idea to substitute or integrate with the traditional and conventional dryers in drying process of medicinal plants.

Solar drying has been proved to be a useful method to preserve the original quality of the product [6]. In recent years, several studies have been done by researches to use the solar dryers for different agricultural and food products such as mint [7], red pepper [8], turmeric (Curcuma longa) [9], rough rice [10], potato [11], and thyme [12]. Lamnatou et al. [13] applied a solar system for apples, carrots, and apricots drying. They found a suitable method for attaining a level of temperature for the warm outlet air using a special collector. Akbulut and Durmuş [14] studied the energy and exergy indices as affected by air flow rate and drying duration. Mehran et al. [4] used a solar dryer in the fluidized-bed mode during the drying process of rough rice grains. They studied the kinetics of drying process, solar energy utilization factor, and drying efficiency. Manrique et al. [15] developed a hybrid solar dryer for coffee beans using the combinative energy of coffee husk pellets combustion and a photovoltaic system and compared the results with those of the conventional method. The uniformity of the products during the drying process has been also investigated using non-destructive methods such as image processing and computational fluid dynamics [16].

An important field of study regarding solar dryers which has been attended by researches is to find the governing mathematical models of the drying operation and to optimize the dryer performance. The most important issues studied in the literature included applying and fitting mathematical models to anticipate and describe the drying behaviour of food products during their dehydration process [12], to evaluate the performance indicators of the developed drying systems such as solar efficiency and solar fraction [17], and to define the optimal working conditions for the proposed solar drying systems [18]. Sami et al. [19] applied several mathematical models to energy and exergy analyses in an indirect solar cabinet dryer. Afriyiye et al. [20] demonstrated that their suggested simulation code could predict temperatures with an error of less than 1.5 %. Akpinar [21] fitted the drying curves of mint leaves to several mathematical models. They reported that "Wang and Singh" model was the superior model to describe the thin-layer drying behavior of mint leaves during forced convection solar drying and natural sun drying. Subbian et al. [18] used Response Surface Methodology to determine the appropriate working conditions of a solar tunnel dryer for drying mango slices with acceptable desirability. The combination of Response Surface Methodology and multi-layered finite element model has also been applied to find the optimal working conditions during simulated solar drying of rough rice grains [22].

A good idea to use solar energy sources in the drying process of food products is to use solar water heaters. One of the advantages of solar water heaters is their ability to save thermal energy so that when there is no sufficient access to solar radiation, it is possible to supply the thermal energy in the form of hot water stored in the solar water heater reservoir. Moreover, by using solar water heaters, it is possible to store thermal energy in the form of a closed cycle for a long time. Several researchers have attempted to benefit from the mentioned advantages of solar water heaters in different application areas. Jahangiri et al. [23] studied the possibility of applying solar water heaters to supply domestic hot water and space heating demands in ten regions of Canada. They found that applying such equipment would lead to an annual reduction of about 984 m^3 in natural gas consumption and 2080 kg in Greenhouse Gas emissions. In another research, Pahlavan et al. [24] indicated that as a result of using solar water heaters in 37 stations in Algeria, considerable amounts of thermal energy of about 100 MWh and 150 MWh could be produced for sanitary hot water and space heating, respectively. The software-based economic analysis demonstrates a significant improvement in the capital return and fossil fuel reduction indices by applying solar water heaters to supply warm water for buildings [25]. The capability of solar water heaters of different types to supply the domestic hot water has been also investigated and proven in Turkey [26] and Zambia [27].

Review of the literature shows that no experimental study has been conducted so far on the performance analysis and optimization of a hybrid solar-assisted multi-belt conveyor dryer including the combination of solar-powered IR lamps and solar water heater in the drying process of stevia leaves. Therefore, in this research, a hybrid solar dryer consisting of a multi conveyor belt drying chamber whose required thermal energy could be supplied with a thermosiphon type solar water heater and four IR lamps was applied for stevia leaves drying. The system is capable of altering the source of thermal energy automatically between the solar and gas water heater based on the drying conditions and information of drying air humidity/temperature sensors. The performance characteristics of the drying system were experimentally evaluated and the optimal working conditions of the dryer were also determined using Response Surface Methodology (RSM).

2. EXPERIMENTAL

2.1. Sample preparation

Fresh stevia leaf samples were provided from Agricultural Biotechnology Research Institute of Iran-North Branch (ABRII), Rasht, Iran. Stevia is known as a natural sweetener with remarkably high sweetness as compared with sugar [28]. The initial moisture content of the leaves was measured based on oven drying method and using the following equation [29]:

$$MC_{d.b.} = \frac{M_i - M_f}{M_f} \times 100 \quad (1)$$

where M_i and M_f are the mass of fresh and dried sample (g), respectively, and $MC_{d.b.}$ is the dry basis moisture content of the product.

2.2. Hybrid solar dryer

A hybrid solar dryer consisting of a multi-conveyor belt drying chamber whose required thermal energy could be supplied with the combination of a thermosiphon type solar water heater, a gas water heater, and four infrared lamps was applied for product drying. The IR lamps were supplied by a photovoltaic system consisting of three 250 W solar panels. More details on the working procedure of the combined gas-solar water heater were reported by [4]. The schematic of the developed drying system is shown in Figure 1. Using a centrifugal blower, the air was passed through a heat exchanger into a cube-shape drying chamber with the dimensions of 150 × 150 × 80 cm^3. The drying chamber

consisted of four belt conveyors which were placed at 20 cm vertical distance with respect to each other. The conveyor belts were of Teflon open mesh type which allowed a continuous and uniform airflow through the samples. Each conveyor moved in the opposite direction to its adjacent conveyor. The conveyors were driven by a 750 W electromotor whose speed was controlled using a variable frequency drive (LS Model IC5, South Korea). The conveyors were run at a constant and low linear speed. They were connected to each other by belt and pulley mechanism. The drying chamber was equipped with four 250 W IR lamps so that one IR lamp was placed above each belt conveyor. The IR lamps were connected together through a series-type electrical circuit. A variable resistor rotary potentiometer was employed to adjust the input power of IR lamps to desired powers.

The power consumption of IR circuit was monitored by a digital Power Meter (Lutron DW-6163, Taiwan). Five digital temperature/relative humidity sensors (AM2301/DHT21, China) were used inside the drying chamber in order to control the inlet air. One of the sensors was placed at the drying chamber inlet port and the other four ones were situated above each conveyor belt. The sensors data were collected and sent to the computer using a microcontroller board. The rotational speed of the centrifugal blower could be adjusted using a variable frequency drive, which was the same type of the one used for driving the conveyor belts electromotor. Afterwards, the inlet air speed could be measured by a digital flowmeter (Lutron YK-80, Taiwan). The overall and internal view of the developed dryer is presented in Figure 2.

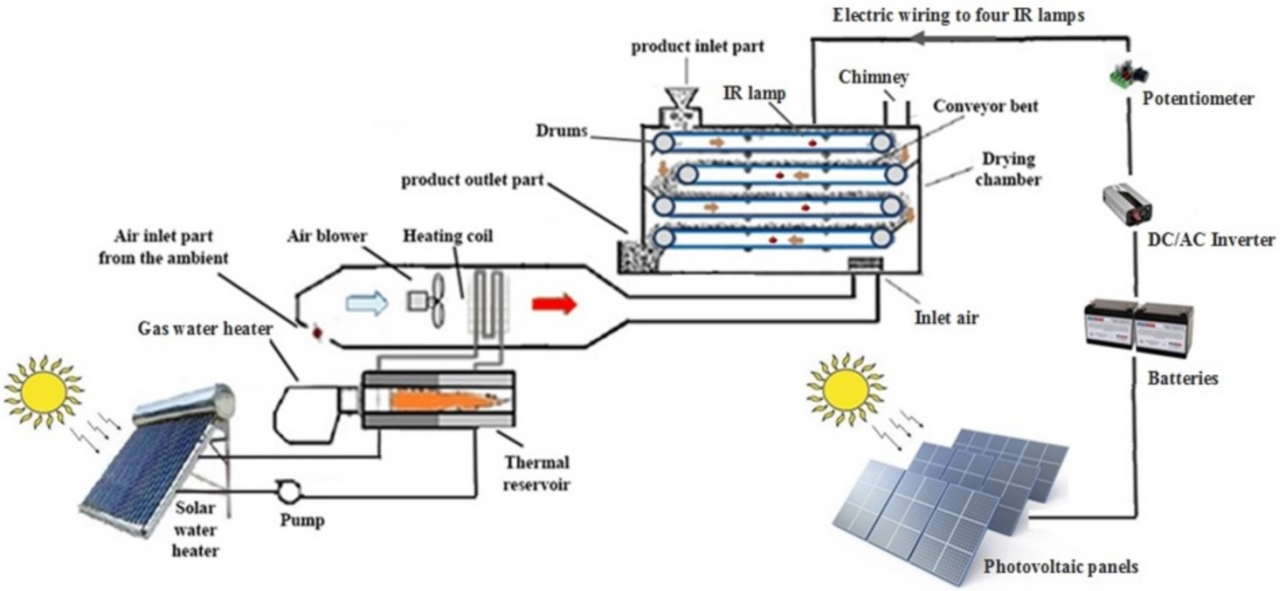

Figure 1. Schematic of the developed solar-assisted dryer working procedure

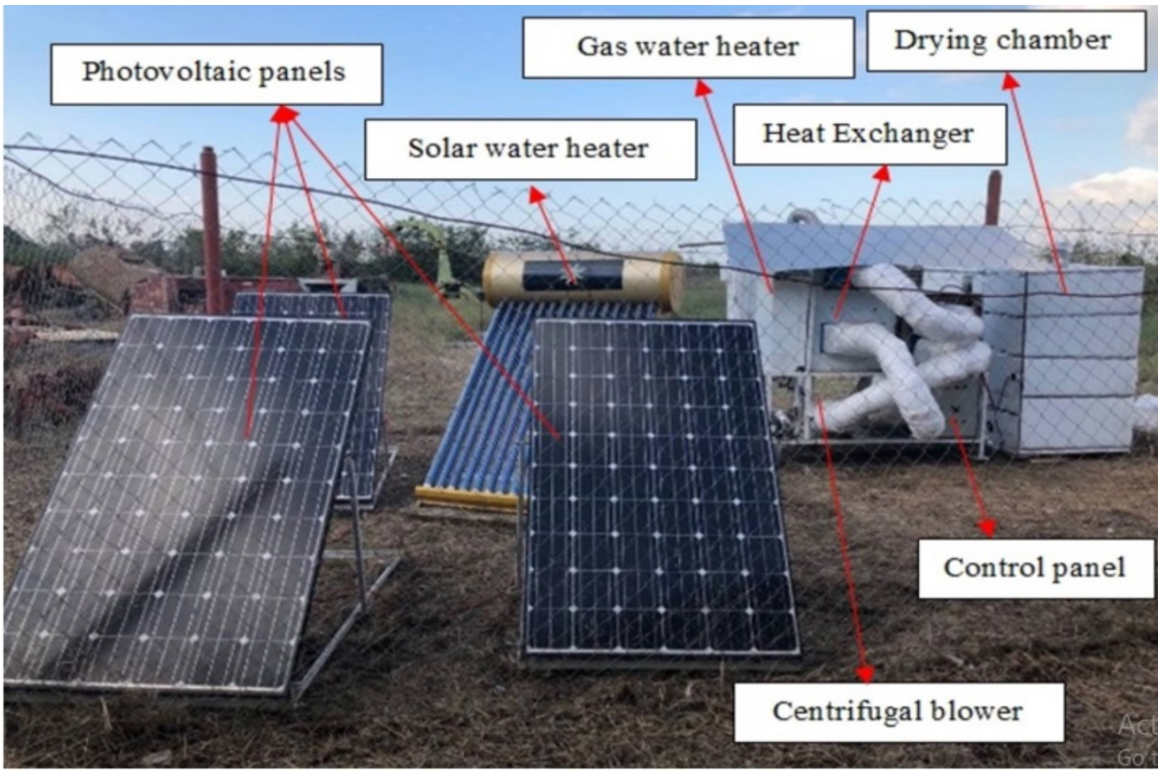

(a)

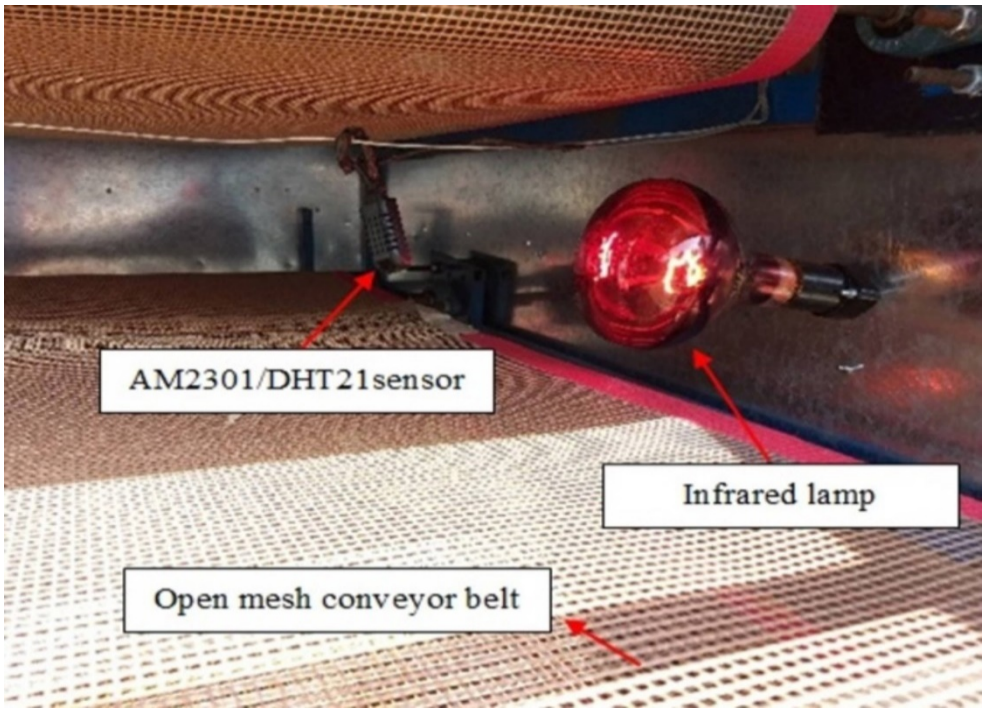

(b)

Figure 2. Experimental setup of the developed drying system: a) Overall view; b) Internal view of drying chamber

2.3. Performance evaluation

The experiments were carried out during July 2019 to September 2019 at the University of Guilan, Rasht, Iran. At each experiment, 300 g of stevia leaves were poured on the highest conveyor in the drying chamber. With the rotation of conveyors, stevia leaves were transferred from the highest conveyor to reach the end part of the lowest conveyor. The goal of the drying process was to dehydrate stevia leaves from a moisture content of about 3.47 (% d.b.) to less than 0.10 (% d.b.). Three factors including drying temperature (30, 40, and 50 °C), inlet air speed (7, 8, and 9 m/s), and infrared power (0, 150, and 300 W) were defined to evaluate the performance of the drying system. The performance indicators included energy consumption, energy efficiency, and drying time. The mentioned indices are defined in the following.

2.3.1. OSE

OSE refers to the total energy used to dehydrate leaves during the drying process. It was calculated as follows [30]:

$$OSE = \frac{E_t}{m_{ew}} \quad (2)$$

where E_t is the overall energy consumed by the dryer (MJ) and mew is the mass of removed water (kg). The E_t value was calculated based on the following formula:

$$E_t = E_{gwh} + E_{swh} + E_{irc} + E_{cb} \quad (3)$$

where E_{gwh} is energy consumption of the gas water heater, E_{swh} is the thermal energy gain of the solar water heater, E_{irc} is energy consumption of infrared lamps, E_{cb} is energy consumption of centrifugal blower, all in terms of MJ, and mew is the mass of removed water (kg).

2.3.1.1. E_{gwh}

E_{gwh} was measured using the following equation [30]:

$$E_{gwh} = V_g \times E_{eq} \quad (4)$$

where V_g is the volume of natural gas consumed by the water heater (m^3) and E_{eq} is the equivalent energy of natural gas (MJ/m^3), which is equal to 8600 kcal or 35.96 MJ/m^3 in Iran [31].

2.3.1.2. E_{swh}

In order to calculate E_{swh}, the following formula was used [32]:

$$E_{swh} = m_w \times c_p \times (T_{fw} - T_{iw}) \quad (5)$$

where m_w is the mass of stored water in the solar heater tank (kg), c_p is water specific heat (J/kgºC), and T_{fw} and T_{iw} are the final and initial temperatures of water (ºC), respectively.

2.3.1.3. E_{cb}

The value of E_{cb} was obtained using the following formula [33]:

$$E_{cb} = \Delta P_t \times Q_a \times t \quad (6)$$

where ΔP is pressure loss (kPa), Q_a volumetric airflow of the blower (m^3/s), and t drying time (s).

2.3.1.4. E_{irc}

The value of consumed energy by IR lamps (E_{irc}) was determined as follows:

$$E_{irc} = P_{ir} \times t \quad (7)$$

where P_{ir} is the power consumed by IR circuit including four IR lamps (W) and t is drying time (s).

In order to calculate mew value in Eq. (2), the following equation was used [34]:

$$m_{ew} = \frac{m_0 \times (MC_0 - MC_f)}{(100 - MC_f)} \quad (8)$$

where m_0 is the mass of fresh leaves (kg) and MC_0 and MC_f are initial and final moisture contents of the leaves, respectively.

2.3.2. NSE

Considering the fact that a part of the required thermal energy was supplied by renewable energy sources, a special energy index was defined to indicate how much fossil fuel as a non-renewable energy source was used for moisture removal in the developed drying system. The difference between OSE and NSE points to the effectiveness of the solar energy usage. Hence, the NSE of the drying system is defined as follows:

$$NSE = \frac{E_{ns}}{m_{ew}} \quad (9)$$

where E_{ns} is the non-solar type of energy (MJ) and was defined via the following equation:

$$E_{ns} = E_{gwh} + E_{cb} \quad (10)$$

2.3.3. OEE

OEE was calculated using the equation below [33]:

$$OEE = \frac{E_e}{E_t} \quad (11)$$

where E_e is moisture evaporation energy for (MJ) and can be obtained as follows [33]:

$$E_e = h_{fg}.m_{ew} \quad (12)$$

In order to calculate the latent heat of vaporization with respect to absolute temperature (T_{abs}), the following equations were applied [33]:

$$h_{fg} = 2.503 \times 10^6 - 2.386 \times 10^3 (T_{abs} - 273.16) \quad (13)$$
$$273.16 \leq T_{abs}(k) \leq 338.72$$

$$h_{fg} = (7.33 \times 10^{12} - 1.60 \times 10^7 {T_{abs}}^2)^{0.5} \quad (14)$$
$$338.72 \leq T_{abs}(k) \leq 533.16$$

2.3.4. SEE

In the calculation of SEE, the solar energy consumption was neglected from the overall input energy of the drying system. In fact, this index was defined to show how much renewable energy sources would be effective in promoting the efficiency of the drying system. The SEE was calculated via the following equation:

$$SEE = \frac{E_e}{E_{ns}} \quad (15)$$

2.4. Modeling and optimization

RSM is known as an applicable method to find the optimal condition of factors interaction. It can also help estimate the optimal process conditions with the least number of experiments [35]. In this research, the Box-Behnken method was used for statistical analyses and to obtain the optimum working conditions for the solar dryer [36]. The related analyses were performed using Design Expert Software (version 11.0.3). Three code levels (-1, 0, +1) were considered for each independent variable (Table 1). The flowchart of RSM applied to the solar drying process is shown in Figure 3.

The optimization process of the drying system was performed considering two working modes. In the first mode (named as overall mode), the energy consumption of both solar and non-solar energy sources was considered in the evaluations. In this mode, three performance characteristics namely drying time, OSE, and OEE were defined as goals in the optimization process. In the second mode (called as solar-assisted mode), only the non-solar energy sources (gas water heater and centrifugal blower) were considered in the system optimization. In this condition, the performance indicators consisted of NSE, SEE, and drying time. The second mode was defined to illustrate the effect of applying renewable energy sources in the drying system.

Table 1. The code levels of independent variables

Independent variable	Coded values		
	-1	0	1
A: Drying air velocity (m/s)	7	8	9
B: Drying air temperature (°C)	30	40	50
C: IR circuit power (W)	0	150	300

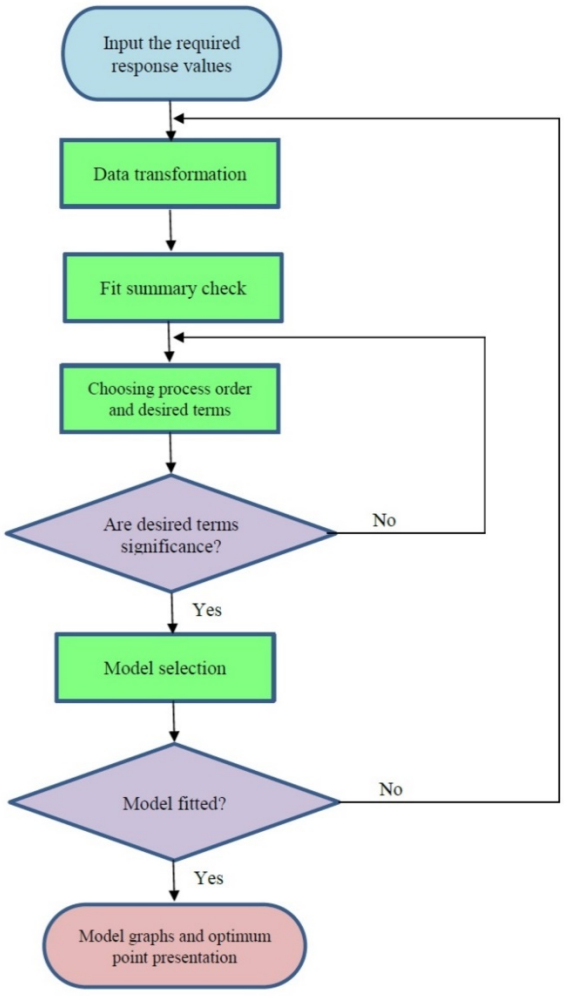

Figure 3. The flowchart of RSM applied to the solar drying process

3. RESULTS AND DISCUSSION

3.1. Overall mode optimization

3.1.1. Statistical analysis

Based on the RSM analysis, 17 working conditions were defined for evaluating the drying system. The results of the experimental tests and the related data predicted by Box-Behnken method are presented in Table 2. Analyses of data indicated that Quadratic model was successfully able to fit the three responses (drying time, OSE, and OEE) versus the independent variables.

Analysis of variance for the three responses together with the coefficient estimates is given in Table 3. The positive sign of the estimated regression coefficients obtained from the model points to the growing influence of the working factors on the responses, while the negative sign coefficients show a decreasing influence on the responses [37]. The magnitude of the coefficients indicates that the related working factor has a greater influence on the responses. The results revealed that the individual factors significantly affected the performance characteristics of the drying system.

3.1.2. Overall drying time

The interaction of "IR power * air temperature" on drying time was statistically significant (p-value < 0.0001). In Figure 4, it can be observed that drying time decreased with the increase of air temperature. Other researchers also reported similar results in this regard [38]. Increasing IR power from 0 to 300 W shortened the drying time. Nevertheless, the slope of the related curve was lower than that of the inlet air temperature. According to Table 2, the lowest value of drying time was 104 minutes which was obtained by applying the combination of 8 m/s * 50 °C * 300 W. The longest time of drying (567 minutes) was obtained upon choosing the values of 8 m/s, 30 °C, and 0 W for the working factors. There are similar researches in the literature that prove the effect of applying radiative IR lamps on the reduction of the drying process time [11].

Table 2. The design points suggested by Box-Behnken method for the experiments and their related experimental and predicted data in overall mode optimization

Run	Independent variables			Real responses (Experiment)			Predicted responses (Model)		
	IR power (W)	Air temperature (ºC)	Air velocity (m/s)	Drying time (min)	Specific energy consumption (MJ/kg water)	Energy efficiency (%)	Drying time (min)	Specific energy consumption (MJ/kg water)	Energy efficiency (%)
1	150	50	9	139	23.67	10.07	137.49	23.92	9.90
2	300	50	8	104	20.74	11.50	116.12	20.85	11.35
3	150	40	8	248	30.15	7.98	249.6	30.18	7.98
4	150	30	9	394	34.85	6.98	395.75	34.15	7.12
5	0	30	8	567	20.78	11.70	554.88	20.67	11.85
6	300	40	7	191	32.21	7.47	180.63	31.38	7.76
7	0	50	8	221	17.60	13.55	212.12	16.53	14.01
8	0	40	7	355	17.30	13.92	365.63	17.66	13.61
9	150	40	8	251	30.27	7.95	249.6	30.18	7.98
10	150	50	7	176	18.70	12.75	174.25	19.41	12.60
11	300	40	9	159	32.95	7.31	148.37	32.58	7.62
12	300	30	8	279	38.29	6.35	287.88	39.35	5.87
13	150	40	8	247	29.84	8.07	249.6	30.18	7.98
14	0	40	9	316	22.48	10.71	326.37	23.30	10.42
15	150	30	7	429	32.06	7.58	430.51	31.82	7.75
16	150	40	8	250	30.25	7.96	249.60	30.18	7.98
17	150	40	8	252	30.39	7.92	249.60	30.18	7.98

Table 3. Analysis of variance of Quadratic model for drying time, overall energy consumption, solar fraction and energy efficiency in overall mode optimization

Source	df	Drying time (min)			Overall specific energy (MJ/kg water)			Overall energy efficiency (%)		
		Sum of squares	F-value[֍]	Coefficient estimate	Sum of squares	F-value	Coefficient estimate	Sum of squares	F-value	Coefficient estimate
Model	9	2.140E+05	180.81**	249.60	682.98	102.00**	30.18	96.39	77.94**	7.98
A	1	65884.50	501.05**	-90.75	264.84	355.98**	5.75	37.19	270.63**	-2.16
B	1	1.324E+05	1006.56**	-128.63	256.28	344.46**	-5.66	29.06	211.45**	1.91
C	1	2556.13	19.44**	-17.88	23.38	31.43**	1.71	5.54	40.33**	-0.8324
AB	1	7310.25	55.59**	42.75	51.65	69.42**	-3.59	2.73	19.84**	0.8257
AC	1	12.25	0.0932^{ns}	1.75	4.96	6.66*	-1.11	2.32	16.87**	0.7612
BC	1	1.0000	0.0076^{ns}	-0.5000	1.18	1.59^{ns}	0.5435	1.07	7.77*	-0.5166
A^2	1	203.38	1.55^{ns}	6.95	50.35	67.68**	-3.46	11.49	83.60**	1.65
B^2	1	5517.64	41.96**	36.20	23.70	31.86**	-2.37	5.51	40.11**	1.14
C^2	1	7.12	0.0541^{ns}	-1.30	0.9994	1.34^{ns}	-0.4872	0.2092	1.52^{ns}	0.2229
Residual	7	920.45			5.21			0.9619		

֍: A-IR power; B-Air temperature; C-Air velocity; ** significant in 1 % probability level; * significant in 5 % probability level; ^{ns}: not statistically significant

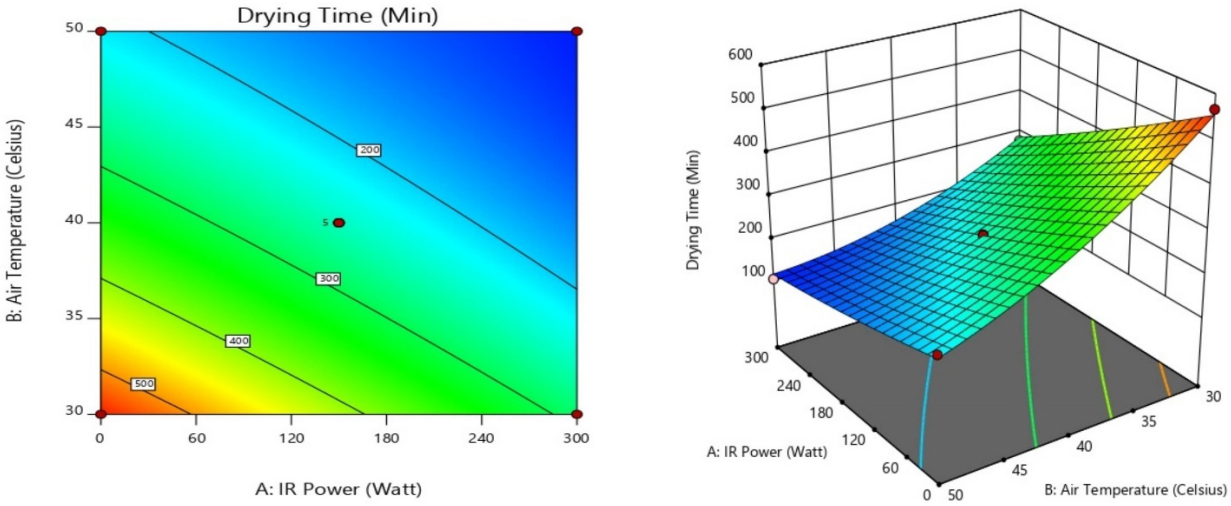

(a) (b)

Figure 4. The interaction effect of IR Power * air temperature on drying time in: a) Contour and b) 3D surface diagrammatic view

3.1.3. OSE

OSE was significantly affected by the interactions of "IR power * air temperature" and "IR power * air speed" at 1 % and 5 % probability levels, respectively. In Figure 5, upon increasing air temperature, a kind of parabolic change with a decreasing approach is made to the amount of OSE. Increasing the IR power similarly causes a parabolically increasing trend in the value of specific energy. The OSE increased with increase in air speed. The result was related to the higher electricity consumption of the centrifugal blower for supplying higher air speeds. The lowest value of OSE (17.30 MJ/kg water evaporated) was obtained by applying the combination of 7 m/s * 40 °C * 0 W, for the inlet air speed, air temperature, and IR power, respectively. The highest OSE (38.29 MJ/kg water evaporated) corresponded to the combination of 8 m/s * 30 °C * 300 W. It has been reported that the energy consumption of a multi-conveyor belt dryer supplied with natural gas ranged from 467.99 to 4607.94 kJ [39].

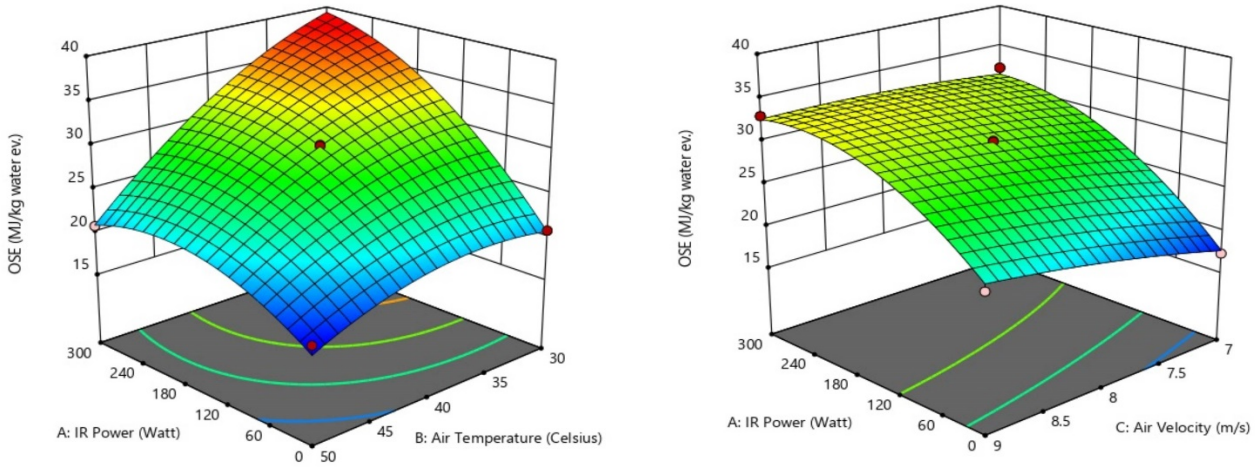

(a) (b)

Figure 5. Interaction effects of: a) IR Power * Inlet air temperature and b) IR Power * Inlet air speed OSE

3.1.4. OEE

OEE is a good indicator to show the overall energy input used for removing extra water from the products in drying systems [30]. The variations of OEE with respect to the interaction of "IR power * air temperature" and "IR power * air speed" are depicted in Figure 6. The aforementioned interaction effects were significant at a 1 % probability level (p-value < 0.0001). It was observed that with increasing IR power from 0 to 300 W, the value of OEE decreased. This indicates that at higher levels of IR power, a greater amount of energy is wasted in the system. It should be noted that this conclusion was derived by supposing the required thermal energy of the dying system to be supplied by only non-solar sources. In other words, if the overall convection and radiant thermal energy of the drying system were provided only by non-solar sources, the OEE decreased by increasing IR power. Increasing the drying air temperature caused the OEE to increase. Meanwhile, OEE decreased by increasing air speed. A similar trend has been reported by other researchers [33]. The highest OEE was 13.92 %, which was obtained by applying the working levels of 7 m/s, 40 °C, and 0 W, whilst the lowest OEE (6.35 %) belonged to the levels of 8 m/s, 30 °C, and 300 W. Sami et al. [19] reported that by applying the air temperature of 69 ºC, the highest values of collector output exergy and energy in their studied indirect solar cabinet dryer were 2.5 kW and 1.12 kW, respectively.

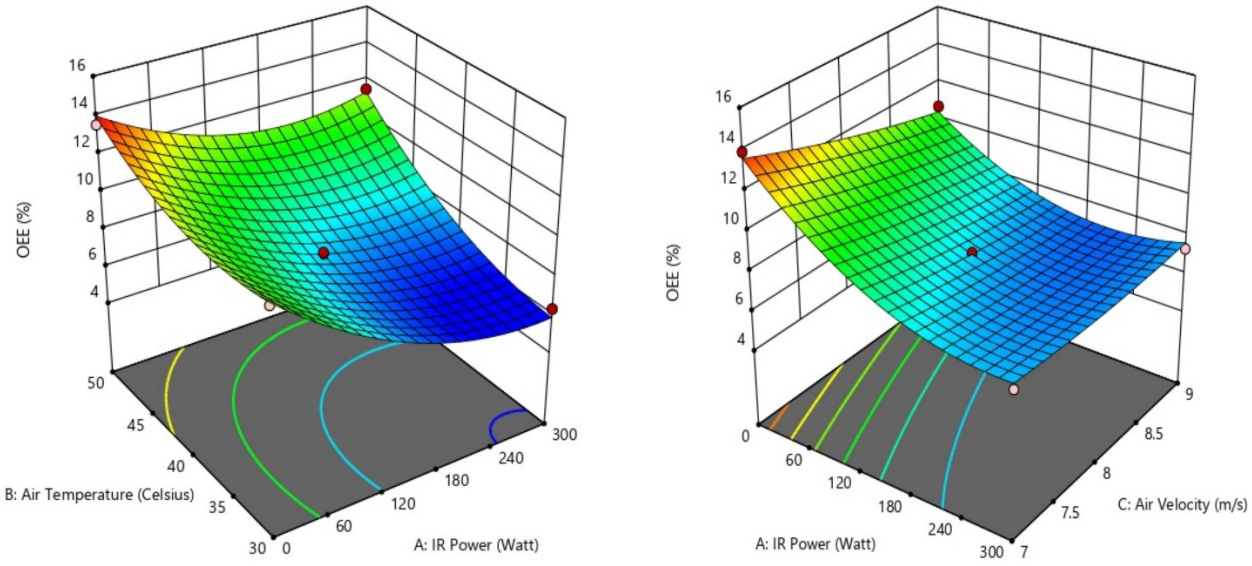

(a) (b)

Figure 6. Interaction effects of: a) Inlet air temperature × IR Power and b) IR Power × Inlet air speed on OEE

3.1.5. Optimum conditions

The working condition of the developed drying system was optimized using the desirability function method in Design Expert software. The goal of the optimization process in the overall mode was to minimize drying time and OSE and to maximize the OEE. Accordingly, 43 points were suggested by the software with desirability values of higher than 0.90. The top ten solutions for the optimization process are presented in Table 4. The first optimum point for the drying system included the IR power of 80.64 W, air temperature of 50 ºC, and air speed of 7 m/s. In such a condition, the values of drying time, OSE, and OEE were 198.74 min, 17.15 MJ/kg water evaporated, and 13.92 %, respectively. As shown in Table 4, in most of the points suggested by RSM, the values of IR power, inlet air speed, and air temperature were close to 80 W, 7 m/s, and 50 ºC, respectively. This finding implies that when the drying system is supplied by non-renewable energy sources, the lower levels of IR power and inlet air speed are desired because of the high energy consumption of the IR circuit and centrifugal blower.

The graphical view of the optimum point with respect to the interaction of "IR power * air temperature" is shown in Figure 7. The optimum points are presented inside a small box in each chart. The values of the responses were normalized so that they varied between 0 as minimum value (blue color) to 1 as maximum value (red color). It can be observed that the optimum point was obtained at lower levels of drying time (blue region), lower levels of OSE (blue region), and higher levels of OEE (red region) with a high level of desirability (red region). Lin et al. [40] evaluated the optimum conditions for dehydration of potato slices in an IR-assisted freeze dryer at an air temperature of 37 °C, slice thickness of 8 mm, and distance of 50 mm from the IR radiation. They reported that the drying process could be successfully optimized through the development of the second-order polynomial model.

Table 4. The top ten suggested optimal working conditions of the drying system in the overall optimization mode

No.	IR power (W)	Drying air temperature (ºC)	Drying air velocity (m/s)	Drying time (min)	Overall specific energy consumption (MJ/kg water evaporated)	Overall energy efficiency (%)	Desirability	
1	80.640	50.000	7.000	198.741	17.155	13.919	0.927	**Selected**
2	77.080	50.000	7.040	199.406	17.151	13.919	0.926	
3	79.374	49.948	7.004	199.551	17.163	13.919	0.926	
4	77.413	49.992	7.000	200.011	17.022	13.995	0.925	
5	75.802	49.995	7.000	200.601	16.948	14.036	0.925	
6	73.505	50.000	7.000	201.428	16.839	14.095	0.924	
7	77.120	49.807	7.000	201.547	17.178	13.923	0.924	
8	72.365	49.997	7.000	201.886	16.790	14.123	0.924	
9	60.118	50.000	7.239	202.455	17.109	13.920	0.923	
10	80.640	49.705	7.000	202.968	17.198	13.919	0.923	

Jafari et al. [41] used RSM for optimizing the drying process of eggplant slices by IR power. The suggested optimum conditions in their research were determined as air speed of 1.14 m/s, IR power of 1500 W, and slice thickness of 4.9 mm. Jha and Tripathy [22] reported that the optimized working conditions during simulated solar drying of rough rice grains included power of 700 W, drying air speed of 3.5 m/s, and grain moisture content of 12 %, which resulted in optimal temperature, milling yield, and drying time of 46 °C, 71.48 %, and 90 min, respectively, and a desirability factor of 0.92.

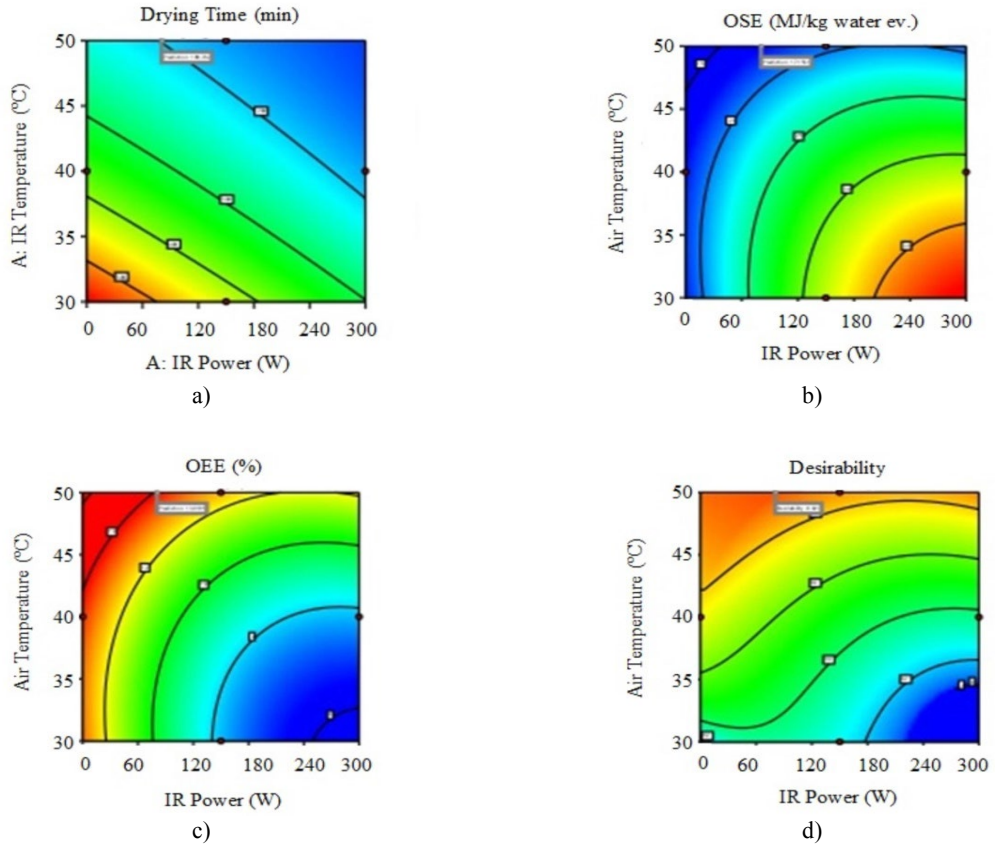

Figure 7. Suggested optimum point in the overall mode based on the combination of working factors for the values of: a) Drying time, b) OSE, c) OEE, and d) Desirability of the optimum point

3.2. Solar-assisted mode optimization

3.2.1. Statistical analysis

In the solar-assisted mode of optimization, the input independent variables for the drying system included IR power, inlet air speed, and air temperature. In this mode, the energy consumption of only non-solar energy sources of the drying system (i.e., gas water heater and centrifugal blower) was considered in the system optimization. The performance indicators of the drying system (responses of the RSM model) consisted of drying time, NSE, and SEE. The 17 working conditions determined by RSM analysis to conduct the experiments and to find the performance indicators of the drying system, together with the corresponding predicted values, are given in Table 5. It can be observed that there is an acceptable accordance between the values of the predicted responses and the experimental data.

The results revealed that the quadratic model based on Box-Behnken method was the superior model to describe the three responses based on the performance factors of the dryer. Table 6 presents the variance analysis of the three responses namely drying time, NSE, and SEE with respect to the three evaluated factors. The coefficient estimates based on the quadratic model are also given. In the solar-assisted optimization mode, all of the three performance indicators of the drying system were significantly influenced by the individual effects of the working factors (Table 6). Among the interaction effects on drying time, only the interaction of "IR power * air temperature" was statistically significant (p-value < 0.0001). The comparison between the predicted data and the actual data in the case of drying time, NSE, and SEE is shown in Figure 8. It can be observed that the values of the model were better fitted to the actual values in the case of drying time than the two other responses. This may be due to the parabolic variation trend of NSE and SEE with respect to independent variables.

Table 5. The design points suggested by Box-Behnken method for the experiments and their related experimental and predicted data in solar-assisted mode optimization

Run	Independent variables			Real responses (Experiment)			Predicted responses (Model)		
	IR Power (W)	Air temperature (ºC)	Air velocity (m/s)	Drying time (min)	NSE (MJ/kg water)	SEE (%)	Drying time (min)	NSE (MJ/kg water)	SEE (%)
1	300	50	8	104	10.84	21.97	116.13	11.61	26.68
2	150	50	7	176	10.20	23.35	174.26	11.09	23.43
3	150	30	9	394	6.13	39.63	395.74	5.25	40.17
4	150	40	8	248	3.44	69.98	249.6	3.47	69.94
5	150	40	8	251	3.56	67.69	249.6	3.47	69.94
6	0	30	8	567	7.70	31.56	554.87	6.93	27.48

7	150	50	9	139	16.99	14.03	137.5	16.15	14.72
8	300	40	7	191	2.71	88.71	180.63	1.08	84.88
9	150	40	8	252	3.67	65.55	249.6	3.47	69.94
10	0	40	9	316	5.08	47.41	326.37	6.72	51.86
11	150	40	8	247	3.13	76.90	249.6	3.47	69.94
12	150	40	8	250	3.54	68.06	249.6	3.47	69.94
13	0	50	8	221	17.60	13.54	212.13	16.78	9.32
14	150	30	7	429	5.00	48.61	430.5	5.83	48.54
15	300	40	9	159	2.91	82.80	148.37	2.98	78.34
16	0	40	7	355	4.20	57.33	365.63	4.14	62.40
17	300	30	8	279	4.48	54.25	287.87	5.30	59.08

Table 6. Analysis of variance of Quadratic model for in solar-assisted mode optimization

Source	df	Drying time (min)			Non-solar specific energy (MJ/kg water)			Solar-assisted energy efficiency (%)		
		Sum of squares	F-value$^{\text{ֆ}}$	Coefficient estimate	Sum of squares	F-value	Coefficient estimate	Sum of squares	F-value	Coefficient estimate
Model	9	2.140E+05	180.81**	+249.60	343.38	24.25**	+3.47	8962.07	29.58**	+69.64
A	1	65884.50	501.05**	-90.75	23.22	14.76**	-1.70	1197.63	35.57**	+12.24
B	1	1.324E+05	1006.56**	-128.63	130.56	82.99**	+4.04	1278.83	37.99**	-12.64
C	1	2556.13	19.44**	-17.88	10.10	6.42*	+1.12	145.65	4.33^{ns}	-4.27
AB	1	7310.25	55.59**	+42.75	3.12	1.98^{ns}	-0.8825	50.78	1.51^{ns}	-3.56
AC	1	12.25	0.0932^{ns}	+1.75	0.1173	0.0746^{ns}	-0.1713	4.02	0.1195^{ns}	+1.00
BC	1	1.0000	0.0076^{ns}	-0.5000	7.97	5.07*	+1.41	0.0294	0.0009^{ns}	-0.0858
A^2	1	203.38	1.55 ^{ns}	+6.95	0.7281	0.4628^{ns}	+0.4158	2.85	0.0847^{ns}	-0.8228
B^2	1	5517.64	41.96**	+36.20	165.76	105.36**	+6.27	6235.07	185.21**	-38.48
C^2	1	7.12	0.0541^{ns}	-1.30	0.1061	0.0675^{ns}	-0.1588	0.2658	0.0079^{ns}	+0.2512
Residual	7	920.45			11.01			235.66		+69.64

$^{\text{ֆ}}$: A-IR power; B-Air temperature; C-Air velocity; ** significant in 1 % probability level; * significant in 5 % probability level; ^{ns}: not statistically significant

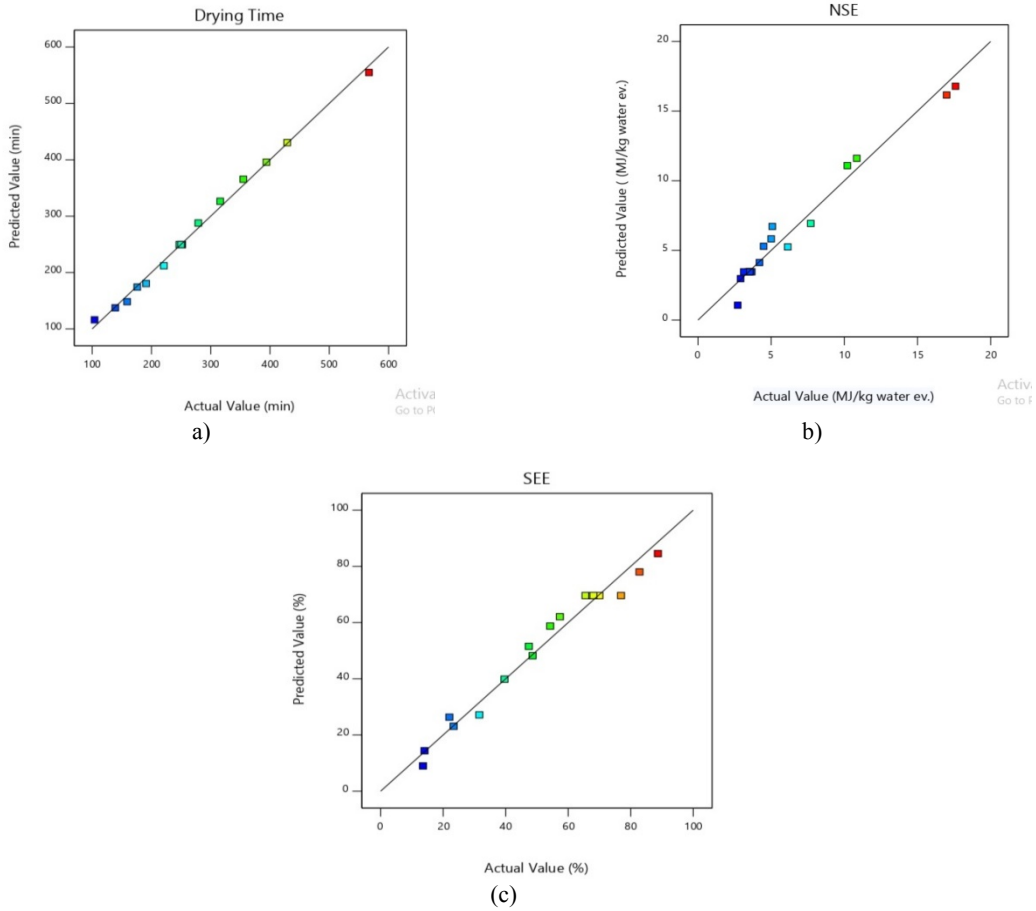

Figure 8. The comparison of the predicted data and the actual data in the case of: a) drying time, b) NSE, and c) SEE

3.2.2. NSE

Variance analysis indicated that the interactions of "IR power × air temperature" and "air temperature × air speed" were significant. The highest NSE was equal to 17.60 MJ/kg water evaporated, which was obtained at an air speed of 8 m/s, air temperature of 50 °C, and IR power of 0 W. The lowest value of NSE (2.71 MJ/kg water evaporated) belonged to the air speed of 7 m/s, air temperature of 40 °C, and IR power of 300 W. The 3D graphical view of the mentioned interaction effect is shown in Figure 9. It can be seen that increasing the drying air temperature resulted in a parabolic increasing trend in the value of NSE. However, with increasing the air speed, the amount of NSE remained at an almost constant level. Increasing the value of NSE at the highest level of drying air temperature was due to the fact that at 50 ºC drying temperature, the thermal energy provided by the solar water heater was not sufficient to complete the drying process. Therefore, at this level of drying temperature, the gas water heater was turned on for a longer time and consequently, the energy consumption increased. Mehran et al. [4] reported that the values of specific energy and solar fraction in their developed solar rough rice dryer ranged from 8 to 22 kWh/kg water and 0.18 to 0.54, respectively. Benhamza et al. [16] indicated that applying an optimized chimney for drying chamber of an indirect solar dryer could decrease the required drying temperature by 7 degrees. In another research, Moghimi et al. [42] developed the performance of a household solar dryer for fruit and vegetables and analysed the dryer using Computational Fluid Dynamics (CFD). Their simulation analyses showed that the drying capacity could be upgraded by more than 50 % by adding a new type tray. According to these findings, one of the future works related to the current study may be the optimization of drying chamber based on analytical methods such as CFD simulations and finite volume method.

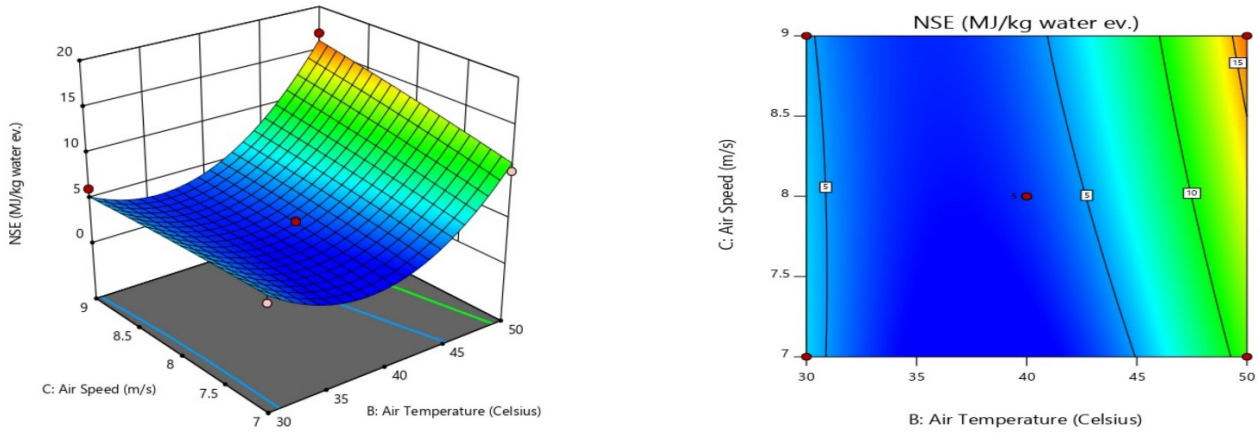

(a) (b)

Figure 9. Variations of NSE considering the interaction effect of Inlet air speed * Inlet air temperature in: a) Contour and b) 3d surface view

3.2.3. SEE

The variations of SEE considering the interaction effects of "air temperature * IR power" and "IR power * air speed" are shown in Figure 10. As can be seen, among the three input variables, IR power and inlet air speed caused a linear variation in the SEE. Compared with the inlet drying temperature of 35 ºC, the SEE increased at a temperature of 45 ºC. By applying 45 ºC temperature, the centrifugal blower worked for a shorter span of time and lower loss in the input energy to the system occurred. The drop in the SEE at the highest temperature level occurred because the gas water heater worked for more time. Subbian et al. [18] reported a decrease in thermal efficiency of their developed solar dryer with increasing drying air temperature.

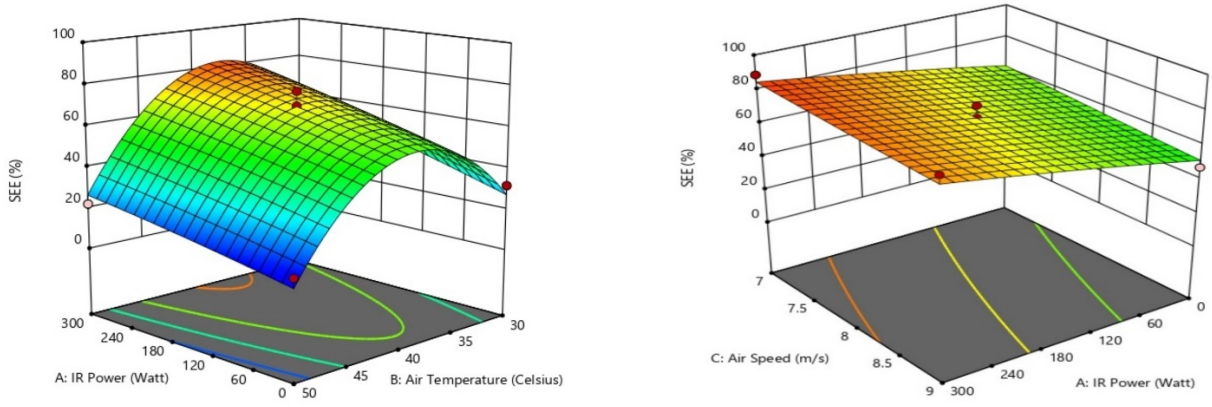

(a) (b)

Figure 10. Interaction effect of a) IR Power * Inlet air temperature and b) Inlet air speed * IR Power on the SEE

The results also revealed that the value of SEE increased with increasing the IR power. In the first optimization mode, it was observed that two different results would be obtained when the drying system gain the IR power in the form of non-solar or solar powered forms. The higher the non-solar powered IR heating, the lower the SEE, while the higher the

solar powered IR heating, the higher the SEE. The highest SEE (88.71 %) was obtained at the levels combination of 7 m/s * 40 °C * 300 W, while the lowest SEE (6.35 %) was attributed to the condition of 8 m/s * 50 °C * 0 W. Manrique et al. [15] reported that approximately 10 % of total electrical energy requirement in their developed dryer could be provided by solar energy. Zoukit et al. [43] reported that the maximum values of energy efficiency in their proposed hybrid solar dryer ranged from 37 to 42 % in different evaluated conditions. Akpinar [21] reported that the energy utilization ratio in their developed drying system ranged from 7.826 % to 46.285 %.

3.2.4. Optimum conditions in solar-assisted mode

The goals of the optimization process in the second working mode were: to minimize the drying time, to minimize the NSE, and to maximize the SEE. In this mode, 68 points were found with desirability values of higher than 0.918. Table 7 presents the top ten solutions for the optimization process. The superior optimum point was obtained in the condition of 300 W * 39.96 ºC * 7 m/s. At this point, the values of drying time, NSE, and SEE were obtained as 180.95 min, 1.062 MJ/kg water, and 84.63 %, respectively. According to Table 7, it can be found that most of suggested working conditions by the optimization process in the solar-assisted mode were close to the point of 300 W * 40 ºC * 7 m/s. In terms of the effectiveness of IR lamps in the drying system, this finding was in contrast with the results of the first optimization mode. In the second optimization mode, which represents the real working conditions of the drying system, it was suggested that the highest level of IR power should be applied in order to achieve a higher drying efficiency. It can also be found that by applying solar-powered IR lamps in the drying system can result in a 10 ºC reduction in the inlet drying temperature, achieving a considerably decreased energy consumption and improved energy efficiency, as compared with the overall optimization mode. The situation of the suggested optimum point versus the evaluated working factors is shown in Figure 11. The applied optimization method was appropriately able to maintain the three responses at their desired levels. In the case of drying time and NSE, the related charts mostly tended to blue color (representing the normalized minimum values), while for the SEE and desirability indices, the optimization plots tended to red colors (maximum regions). It can also be observed that the optimization plot of the NSE was more filled with blue color than the OSE chart (Figure 5b). This shows that by using solar energy in the drying process, wider combinations of the working factors could be applied to achieve lower fossil energy consumption. According to the findings of this research, it is concluded that the application of the developed drying system can result in a remarkable reduction in the need for fossil fuel sources and consequently, a considerable decrease in the amount of greenhouse gases emission into the atmosphere. In recent years, several researchers have investigated the application of solar energy to drying systems of agricultural crops as well as optimization of the drying systems. Suzihaque and Driscoll [44] developed a solar dryer for coffee beans with the ability of heat recovery and optimized the dryer dimensions based on heat and mass transfer models. They concluded that the optimum values of the dryer height and length and coffee bed thickness were equal to 0.4030 m, 0.7920 m, and 0.0278 m, respectively. Sethi and Dhiman [45] developed a hybrid greenhouse dryer for fenugreek drying by combination of solar-biomass energy. Optimization process demonstrates that to have a drying air temperature of 32.3-62.4 ºC, the heating requirements of the dryer may range from 0.348 to 12.18 kW.

Table 7. The top ten suggested optimal working conditions of the drying system in the solar-assisted optimization mode

No.	IR power (W)	Drying air temperature (ºC)	Drying air velocity (m/s)	Drying time (min)	NSE (MJ/kg water evaporated)	Solar-assisted energy efficiency (%)	Desirability	
1	300.000	39.961	7.000	180.955	1.062	84.626	0.924	**Selected**
2	300.000	39.846	7.002	181.924	1.046	84.797	0.924	
3	299.998	39.983	7.008	180.661	1.076	84.561	0.924	
4	300.000	39.869	7.015	181.548	1.066	84.713	0.924	
5	300.000	39.732	7.000	182.938	1.027	84.969	0.924	
6	300.000	39.917	7.031	180.921	1.093	84.581	0.924	
7	300.000	39.902	7.040	180.924	1.103	84.569	0.924	
8	299.718	40.073	7.000	180.148	1.084	84.426	0.924	
9	299.998	39.927	7.051	180.565	1.120	84.491	0.924	
10	299.999	39.491	7.000	185.069	0.996	85.286	0.923	

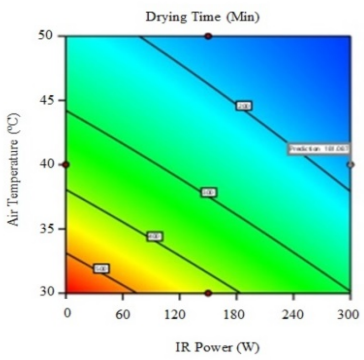

a)

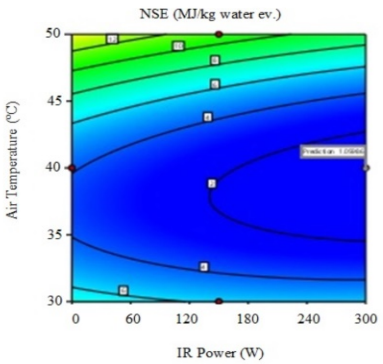

b)

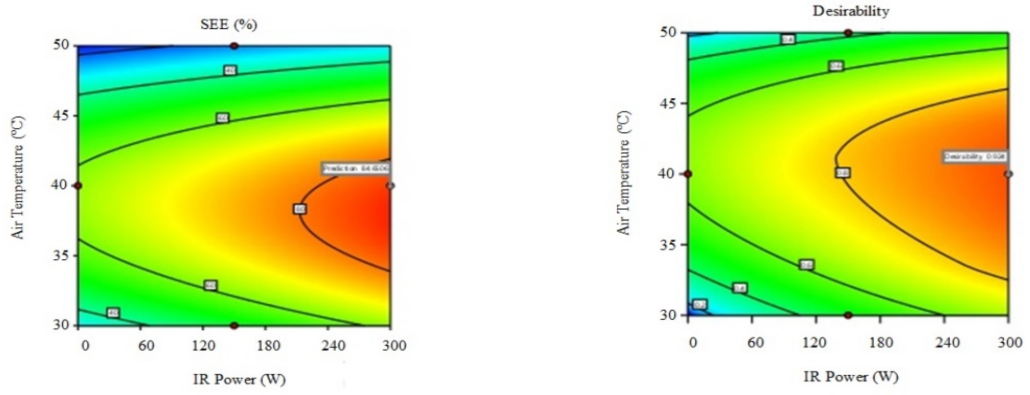

c) d)

Figure 11. Suggested optimum point in the solar-assisted mode based on the combination of working factors for the values of: a) Drying time, b) NSE, c) SEE, and d) Desirability of the optimum point

4. CONCLUSIONS

In this study, the energy efficiency and performance characteristics of a solar-assisted multi-belt conveyor dryer were evaluated experimentally. The RSM-based optimization process was performed considering two general working modes for the drying system. In the first mode (named as the overall mode), the energy consumption of both solar and non-solar energy sources was considered in the analyses. In the second mode (called as solar-assisted mode), only the non-solar energy sources (gas water heater and centrifugal blower) were considered in the system optimization. According to the results obtained, the following conclusions were derived:

- The increase in the inlet temperature resulted in a kind of parabolic change with a decreasing trend in the value of OSE. Increasing the IR power similarly caused a parabolic change in the specific energy. However, the trend of variations in this case increased.
- It was observed that upon increasing IR power, the OEE decreased. This indicates that at the higher levels of non-solar IR power, a more amount of energy was wasted in the system. The value of OEE increased upon increasing the inlet temperature.
- Depending on whether the dryer gains the IR power in the form of non-solar or solar powered forms, two different results can be obtained. The higher the non-solar powered IR heating, the lower the energy efficiency, while the higher the solar powered IR heating, the higher the energy efficiency.
- The overall comparison between the values of OEE and SEE indicated that the variation of OEE versus the inlet temperature was increasing and approximately linear, while the SEE had a parabolic increasing trend with respect to the increased temperature.
- The value of OEE in the drying system ranged from 5.87 to 14.01 %, whilst the SEE during the experiments was obtained in the range of 9.32-84.88 %. The considerable difference between the values of OEE and SEE is a good indicator to illustrate the effect of renewable energy sources in the second optimization mode. In other words, in the second optimization mode, the lower amounts of fuel-based energy sources were used for moisture removal from the product. This finding can lead to a significant improvement in the process cost, energy consumption, and efficiency in the long term.
- The majority of the suggested working conditions by the optimization process in the solar-assisted mode corresponded to the treatment of 300 W * 40 ºC * 7 m/s. This finding was in contrast with the results of the first optimization mode in terms of the effectiveness of IR lamps in the drying system. In the second optimization mode, which represents the real working conditions of the drying system, it was suggested that in order to have a higher drying efficiency, the highest level of IR power should be applied.
- Comparison of the optimum points suggested that by using RSM in the two defined optimization modes, it was found that applying solar-powered IR lamps in the drying system could result in a 10 ºC reduction in the inlet drying temperature while achieving considerably decreased energy consumption and improved energy efficiency, as compared with the overall optimization mode.
- According to the findings of this research, it is concluded that the application of the developed drying system can result in a remarkable reduction in the need for fossil fuel sources that can consequently cause a decrease in the amount of greenhouse gases emission into the atmosphere. The developed drying system may also be converted into a very low or even zero fossil energy consuming dryer if the centrifugal blower is powered by solar-based electrical energy.
- One of the working limitations of the proposed drying system was the unpredictability of the prevailing weather conditions in the region of study so that the thermal energy generation capacity of the solar system might be affected by occasional cloudiness. However, thanks to the capability of the proposed system to store the thermal energy in the water heater reservoir and solar panel batteries, it was made possible to supply a considerable part of the required heat in such conditions.
- Since previous studies have demonstrated that the application of an optimized chimney for drying chamber of solar dryers could decrease the required drying temperature and thermal energy, the future works may be focused on the optimization of the system drying chamber based on analytical methods such as computational fluid dynamics. Moreover, the development of an automated control system for the dryer to instantaneously monitor and adjust the major working parameters of the drying process can be one of the other future areas of interest.

5. ACKNOWLEDGEMENT

The authors would like to thank the University of Guilan for financially support of this research under grant number of 128234.

NOMENCLATURE

ΔP	Total pressure drop (kPa)
c_p	Specific heat of water (J/kg ºC)
E_{cb}	Energy consumption of the centrifugal blower (MJ)
E_e	Energy required for moisture evaporation (MJ)
E_{eq}	Energy equivalent of natural gas (MJ/m^3)
E_{gwh}	Energy consumption of the gas water heater (MJ)
E_{irc}	Energy consumption of IR circuit (MJ)
E_{ns}	Non-solar type of energy consumed by the drying system (MJ)
E_{swh}	Energy consumption of solar water heater (MJ)
E_t	Overall energy consumed by the drying system (MJ)
h_{fg}	Latent heat of vaporization (MJ/kg)
i	Number of variables
IR	Infrared
m_0	Initial mass of the product (kg)
MC_0	Initial moisture content of the product (%)
$MC_{d.b.}$	Product moisture based on the dry mass (% d.b.)
MC_f	Final moisture content of the product (%)
m_{ew}	Mass of water evaporated during the drying process (kg)
M_f	Final mass of dried sample (g)
M_i	Initial mass of sample (g)
m_w	Mass of water in the tank (kg)
NSE	Non-solar specific energy (MJ)
OSE	Overall specific energy (MJ)
OEE	Overall energy efficiency (MJ)
P_{ir}	Power consumed by IR circuit (W)
Q_a	Volumetric airflow of blower (m^3/s)
RSM	Response Surface Methodology
SEE	Solar-assisted energy efficiency (MJ)
t	Drying time (s)
T_{fw}	Final temperature of water (ºC)
T_{iw}	Initial temperature of water (ºC)
V_g	Volume of consumed natural gas by the water heater (m^3)
X_i	Coded (independent) variable
X_j	Dependent variable
Y_i	Estimated response
β_{ij}	Constant of variables interaction
β_j	Variables constant
β_{jj}	Constant of second-order parameter
β_o	Model constant
ε	Random error

REFERENCES

1. Lingayat, A.B., Chandramohan, V., Raju, V. and Meda, V., "A review on indirect type solar dryers for agricultural crops–Dryer setup, its performance, energy storage and important highlights", ***Applied Energy***, Vol. 258, (2020), 114005. (https://doi.org/10.1016/j.apenergy.2019.114005).
2. El Hage, H., Herez, A., Ramadan, M., Bazzi, H. and Khaled, M., "An investigation on solar drying: A review with economic and environmental assessment", ***Energy***, Vol. 157, (2018), 815-829. (https://doi.org/10.1016/j.energy.2018.05.197).
3. Sagar, V. and Kumar, P.S., "Recent advances in drying and dehydration of fruits and vegetables: A review", ***Journal of Food Science and Technology***, Vol. 47 No. 1, (2010), 15-26. (https://dx.doi.org/10.1007%2Fs13197-010-0010-8).
4. Mehran, S., Nikian, M., Ghazi, M., Zareiforoush, H. and Bagheri, I., "Experimental investigation and energy analysis of a solar-assisted fluidized-bed dryer including solar water heater and solar-powered infrared lamp for paddy grains drying", ***Solar Energy***, Vol. 190, (2019), 167-184. (https://doi.org/10.1016/j.solener.2019.08.002).
5. Jin, W., Mujumdar, A.S., Zhang, M. and Shi, W., "Novel drying techniques for spices and herbs: A review", ***Food Engineering Reviews***, Vol. 10, No. 1, (2018), 34-45. (https://doi.org/10.1007/s12393-017-9165-7).
6. Lakshmi, D., Muthukumar, P., Layek, A. and Nayak, P.K., "Performance analyses of mixed mode forced convection solar dryer for drying of stevia leaves", ***Solar Energy***, Vol. 188, (2019), 507-518. (https://doi.org/10.1016/j.solener.2019.06.009).
7. Eltawil, M.A., Azam, M.M. and Alghannam, A.O., "Energy analysis of hybrid solar tunnel dryer with PV system and solar collector for drying mint (MenthaViridis)", ***Journal of Cleaner Production***, Vol. 181, (2018), 352-364. (https://doi.org/10.1016/j.jclepro.2018.01.229).
8. Hamdi, I., ELkhadraoui, A., Kooli, S., Farhat, A. and Guizani, A., "Drying of red pepper slices in a solar greenhouse dryer and under open sun: Experimental and mathematical investigations", ***Innovative Food Science & Emerging Technologies***, (2019). (https://doi.org/10.1016/j.ifset.2019.01.001).
9. Karthikeyan, A. and Murugavelh, S., "Thin layer drying kinetics and exergy analysis of turmeric (Curcuma longa) in a mixed mode forced convection solar tunnel dryer", ***Renewable Energy***, Vol. 128, (2018), 305-312. (https://doi.org/10.1016/j.renene.2018.05.061).
10. Yahya, M., Fudholi, A. and Sopian, K., "Energy and exergy analyses of solar-assisted fluidized bed drying integrated with biomass furnace", ***Renewable Energy***, Vol. 105, (2017), 22-29. (https://doi.org/10.1016/j.renene.2016.12.049).
11. Ziaforoughi, A. and Esfahani, J.A., "A salient reduction of energy consumption and drying time in a novel PV-solar collector-assisted intermittent infrared dryer", ***Solar Energy***, Vol. 136, (2016), 428-436. (https://doi.org/10.1016/j.solener.2016.07.025).
12. El-Sebaii, A. and Shalaby, S., "Experimental investigation of an indirect-mode forced convection solar dryer for drying thymus and mint", ***Energy Conversion and Management***, Vol. 74, (2013), 109-116. (https://doi.org/10.1016/j.enconman.2013.05.006).
13. Lamnatou, C., Papanicolaou, E., Belessiotis, V. and Kyriakis, N., "Experimental investigation and thermodynamic performance analysis of a solar dryer using an evacuated-tube air collector", ***Applied Energy***, Vol. 94, (2012), 232-243. (https://doi.org/10.1016/j.apenergy.2012.01.025).
14. Akbulut, A. and Durmuş, A., "Energy and exergy analyses of thin layer drying of mulberry in a forced solar dryer", ***Energy***, Vol. 35, No. 4, (2010), 1754-1763. (https://doi.org/10.1016/j.energy.2009.12.028).
15. Manrique, R., Vásquez, D., Chejne, F. and Pinzón, A., "Energy analysis of a proposed hybrid solar–biomass coffee bean drying system", ***Energy***, (2020), 117720. (https://doi.org/10.1016/j.energy.2020.117720).
16. Benhamza, A., Boubekri, A., Atia, A., Hadibi, T. and Arıcı, M., "Drying uniformity analysis of an indirect solar dryer based on computational fluid dynamics and image processing", ***Sustainable Energy Technologies and Assessments***, Vol. 47, (2021), 101466. (https://doi.org/10.1016/j.seta.2021.101466).
17. Atalay, H., Coban, M.T. and Kıncay, O., "Modeling of the drying process of apple slices: Application with a solar dryer and the thermal energy storage system", ***Energy***, Vol. 134, (2017), 382-391. (https://doi.org/10.1016/j.energy.2017.06.030).
18. Subbian, V., Kumar, S.S., Chaithanya, K., Arul, S.J., Kaliyaperumal, G. and Adam, K.M., "Optimization of solar tunnel dryer for mango slice using response surface methodology", ***Materials Today: Proceedings***, Vol. 46, (2021). (https://doi.org/10.1016/j.matpr.2021.02.382).
19. Sami, S., Etesami, N. and Rahimi, A., "Energy and exergy analysis of an indirect solar cabinet dryer based on mathematical modeling results", ***Energy***, Vol. 36, No. 5, (2011), 2847-2855. (https://doi.org/10.1016/j.energy.2011.02.027).
20. Afriyie, J.K., Rajakaruna, H., Nazha, M.A. and Forson, F., "Mathematical modelling and validation of the drying process in a chimney-dependent solar crop dryer", ***Energy Conversion and Management***, Vol. 67, (2013), 103-116. (https://doi.org/10.1016/j.enconman.2012.11.007).
21. Akpinar, E.K., "Drying of mint leaves in a solar dryer and under open sun: Modelling, performance analyses", ***Energy Conversion and Management***, Vol. 51, No. 12, (2010), 2407-2418. (https://doi.org/10.1016/j.enconman.2010.05.005).
22. Jha, A. and Tripathy, P., "Optimization of process parameters and numerical modeling of heat and mass transfer during simulated solar drying of paddy", ***Computers and Electronics in Agriculture***, Vol. 187, (2021), 106215. (https://doi.org/10.1016/j.compag.2021.106215).

23. Jahangiri, M., Alidadi Shamsabadi, A. and Saghaei, H., "Comprehensive evaluation of using solar water heater on a household scale in Canada", ***Journal of Renewable Energy and Environment (JREE)***, Vol. 5, No. 1, (2018), 35-42. (https://dx.doi.org/10.30501/jree.2018.88491).
24. Pahlavan, S., Jahangiri, M., Alidadi Shamsabadi, A. and Khechekhouche, A., "Feasibility study of solar water heaters in Algeria, A review", ***Journal of Solar Energy Research***, Vol. 3, No. 2, (2018), 135-146. (https://jser.ut.ac.ir/article_67424.html).
25. Zaniani, J.R., Dehkordi, R.H., Bibak, A., Bayat, P. and Jahangiri, M., "Examining the possibility of using solar energy to provide warm water using RETScreen4 software (Case study: Nasr primary school of pirbalut)", ***Current World Environment***, Vol. 10, (2015), 835. (http://dx.doi.org/10.12944/CWE.10.Special-Issue1.101).
26. Siampour, L., Vahdatpour, S., Jahangiri, M., Mostafaeipour, A., Goli, A., Alidadi Shamsabadi, A. and Atabani, A., "Techno-enviro assessment and ranking of Turkey for use of home-scale solar water heaters", ***Sustainable Energy Technologies and Assessments***, Vol. 43, (2021), 100948. (https://doi.org/10.1016/j.seta.2020.100948).
27. Jahangiri, M., Akinlabi, E.T. and Sichilalu, S.M., "Assessment and modeling of household-scale solar water heater application in Zambia: Technical, environmental, and energy analysis", ***International Journal of Photoenergy***, (2021). (https://doi.org/10.1155/2021/6630338).
28. Periche, A., Castelló, M.L., Heredia, A. and Escriche, I., "Influence of drying method on steviol glycosides and antioxidants in Stevia rebaudiana leaves", ***Food Chemistry***, Vol. 172, (2015), 1-6. (https://doi.org/10.1016/j.foodchem.2014.09.029).
29. ASABE, "Moisture measurement—Unground grain and seeds", American Society of Agricultural and Biological Engineers, (2019).
30. Firouzi, S., Alizadeh, M.R. and Haghtalab, D., "Energy consumption and rice milling quality upon drying paddy with a newly-designed horizontal rotary dryer", ***Energy***, Vol. 119, (2017), 629-636. (https://doi.org/10.1016/j.energy.2016.11.026).
31. Sharifi, H., Babapour, Sh. and Sherkati, Sh., "Evaluation of problems caused by thermal degradation of consumed gas in Iran's thermal power stations", Tehran, Iran, (2004).
32. Ceylan, I., "Energy and exergy analyses of a temperature controlled solar water heater", ***Energy and Buildings***, Vol. 47, (2012), 630-635. (https://doi.org/10.1016/j.enbuild.2011.12.040).
33. Tohidi, M., Sadeghi, M. and Torki-Harchegani, M., "Energy and quality aspects for fixed deep bed drying of paddy", ***Renewable and Sustainable Energy Reviews***, Vol. 70, (2017), 519-528. (https://doi.org/10.1016/j.rser.2016.11.196).
34. Anum, R., Ghafoor, A. and Munir, A., "Study of the drying behavior and performance evaluation of gas fired hybrid solar dryer", ***Journal of Food Process Engineering***, Vol. 40, No. 2, (2017), 12351. (https://doi.org/10.1111/jfpe.12351).
35. Myers, R.H., Montgomery, D.C. and Anderson-Cook, C.M., Response surface methodology: Process and product optimization using designed experiments, John Wiley & Sons, (2016). (https://www.wiley.com/en-us/Response+Surface+Methodology%3A+Process+and+Product+Optimization+Using+Designed+Experiments%2C+4th+Edition-p-9781118916018).
36. Yang, Z.-H., Huang, J., Zeng, G.-M., Ruan, M., Zhou, C.-S., Li, L. and Rong, Z.G., "Optimization of flocculation conditions for kaolin suspension using the composite flocculant of MBFGA1 and PAC by response surface methodology", ***Bioresource Technology***, Vol. 100, No. 18, (2009), 4233-4239. (https://doi.org/10.1016/j.biortech.2008.12.033).
37. Chen, X., Du, W. and Liu, D., "Response surface optimization of biocatalytic biodiesel production with acid oil", ***Biochemical Engineering Journal,*** Vol. 40, No. 3, (2008), 423-429. (https://doi.org/10.1016/j.bej.2008.01.012).
38. Singh, G.D., Sharma, R., Bawa, A. and Saxena, D., "Drying and rehydration characteristics of water chestnut (Trapa natans) as a function of drying air temperature", ***Journal of Food Engineering***, Vol. 87, No. 2, (2008), 213-221. (https://doi.org/10.1016/j.jfoodeng.2007.11.027).
39. Soodmand-Moghaddam, S., Sharifi, M. and Zareiforoush, H., "Investigation of fuel consumption and essential oil content in drying process of lemon verbena leaves using a continuous flow dryer equipped with a solar pre-heating system", ***Journal of Cleaner Production***, Vol. 233, (2019), 1133-1145. (https://doi.org/10.1016/j.jclepro.2019.06.083).
40. Lin, Y.P., Lee, T.Y., Tsen, J.H. and King, V.A.E., "Dehydration of yam slices using FIR-assisted freeze drying", ***Journal of Food Engineering***, Vol. 79, No. 4, (2007), 1295-1301. (https://doi.org/10.1016/j.jfoodeng.2006.04.018).
41. Jafari, F., Movagharnejad, K. and Sadeghi, E., "Infrared drying effects on the quality of eggplant slices and process optimization using response surface methodology", ***Food Chemistry***, (2020), 127423. (https://doi.org/10.1016/j.foodchem.2020.127423).
42. Moghimi, P., Rahimzadeh, H. and Ahmadpour, A., "Experimental and numerical optimal design of a household solar fruit and vegetable dryer", ***Solar Energy***, Vol. 214, (2021), 575-587. (https://doi.org/10.1016/j.solener.2020.12.023).
43. Zoukit, A., El Ferouali, H., Salhi, I., Doubabi, S. and Abdenouri, N., "Simulation, design and experimental performance evaluation of an innovative hybrid solar-gas dryer", ***Energy***, Vol. 189, (2019), 116279. (https://doi.org/10.1016/j.energy.2019.116279).
44. Suzihaque, M. and Driscoll, R., "Effects of solar radiation, buoyancy of air flow and optimization study of coffee drying in a heat recovery dryer", ***Procedia Engineering***, Vol. 148, (2016), 812-822. (https://doi.org/10.1016/j.proeng.2016.06.617).
45. Sethi, V. and Dhiman, M., "Design, space optimization and modelling of solar-cum-biomass hybrid greenhouse crop dryer using flue gas heat transfer pipe network", ***Solar Energy***, Vol. 206, (2020), 120-135. (https://doi.org/10.1016/j.solener.2020.06.006).